M. OH*[†], H.K. YU*[†], J.-H. LEE*, M.C. OH*, S.-H. JUNG**, B. AHN*[#]

QUANTITATIVE ANALYSIS OF CRYOMILLED NANOCRYSTALLINE Ti-6Al-4V ALLOY POWDER
BY X-RAY DIFFRACTION

A nanocrystalline Ti alloy powder was fabricated using cryomilling. The grain size and lattice strain evolution during cryomilling were quantitatively analyzed using X-ray diffraction (XRD) based on the Scherrer equation, Williamson-Hall (W-H) plotting method, and size-strain (S-S) method assuming uniform deformation. Other physical parameters including stress and strain have been calculated. The average crystallite size and the lattice strain evaluated from XRD analysis are in good agreement with the result of transmission electron microscopy (TEM).

Keywords: nanocrystalline, cryomilling, Ti alloy, X-ray diffraction, size-strain plot method

1. Introduction

Nanocrystalline (NC) materials with a range of nanoscale microstructure have attracted a great attention due to the unique combination of mechanical and physical properties, which are reportedly superior to those of their coarse-grained counterparts [1-5]. As one of methods to achieve NC microstructure, the cryomilling process has attracted considerable interests due primarily to its ability to generate nanocrystals and other non-equilibrium structures in large quantities. It has also been used to synthesize nanostructured Ti powder [6-12]. The microstructural evolution and grain size refinement during cryomilling involves three steps: (i) local deformation of the shear band increasing of dislocation density, (ii) dislocation annihilation and re-alignment forming low-angle subgrain boundaries, and (iii) development of randomly oriented grains. Cryomilling technique has several characteristics distinguished from conventional mechanical milling processes, such as relatively high strain rates, large cumulative strains, and cryogenic temperature suppressing recovery during milling process. All these characteristics facilitate the grain refinement and reduce time to achieve NC structure [13-15].

To quantitatively analyze nanoscale grains obtained through cryomilling, there is a method of calculating the grain size using broadening of X-ray diffraction peaks scattered by the nanoscale grain boundaries [16]. The Scherrer method is a well-known technique to predict the size of crystallites. However, it is also well known that the grain size obtained using Scherrer method is less accurate because it does not consider the presence of

dislocation and the lattice strain caused by dislocations. In this study, grain size was estimated using the Williamson-Hall (W-H) plot method and size-strain (S-S) plot method. The W-H plot method is based on the Scherrer equation, but it adds a concept of parameters according to the structure and potential of the lattice. In W-H plot method, the parameters are selected using the Fourier technique and the Rietveld refinement, and the grain size and the contribution of the lattice strain are separately measured at the peak broadening. The S-S plot is a similar method to the W-H plot method, but it uses additional functions to calibrate the grain size calculation.

2. Experimental

Commercial purity Ti powder and pre-alloyed 60Al-40V (wt.%) powder were mixed using 3D Tubular mixer to form the final composition of Ti-6Al-4V (wt.%). The powder mixture was cryomilled at a temperature of –160°C and rotation speed of 180 RPM for 4, 6, 8, and 12 hours. For cryomilling, stainless steel vessel and balls about 5 mm in diameter were used with a ball-to-powder weight ratio of 30:1. Prior to cryomilling, about 2 wt.% of stearic acid was added as a process control agent (PCA) in order to suppress the excessive agglomeration of powders.

X-ray diffraction (XRD) analysis was conducted using a D/max-2500V/PC X-ray diffractometer using Cu Kα (λ = 0.15406 nm) radiation. A low scanning rate of 1°/min and a step time of 2 s were used for phase identification and grain

* AJOU UNIVERSITY, DEPARTMENT OF MATERIALS SCIENCE AND ENGINEERING AND DEPARTMENT OF ENERGY SYSTEMS RESEARCH, 206 WORLDCUP-RO, YEONGTONG-GU, SUWON, GYEONGGI, 16499, KOREA
** THE 4TH RESEARCH AND DEVELOPMENT, AGENCY FOR DEFENSE DEVELOPMENT, DAEJEON, KOREA
† THESE AUTHORS CONTRIBUTED EQUALLY TO THIS WORK

Corresponding author: byungmin@ajou.ac.kr

1440

size measurements. For instrumental correction of XRD peak broadening, Gaussian-Gaussian relationship was used [17]:

$$\beta_{exp}^2 = \beta^2 + \beta_{ins}^2 \tag{1}$$

where β is the measured FWHM and β_{ins} is the FWHM of the Fully Annealed powder. TEM observations were carried out using a FEI Tecnai G2 F30 S-Twin microscope operated at 200 kV. The samples were prepared by embedding the powders in GATAN G-1 epoxy, followed by mechanical polishing, dimpling, and ion milling.

3. Results and discussion

Figure 1 shows XRD patterns of cryomilled powders with different milling times. Mainly detectable peaks are indexed as alpha Ti structure (JCPDS No. 44-1294). But some other minor peaks marked with black dots in Fig. 1 are also observed which are indexed as Al-3V structure (JCPDS No. 07-0309). The weight ratio of 60Al-40V powder is 10%, but the intensity ratio of Al-3 V peak was less than 10%. This result indicates that the Al-V compound is still remain in powder without phase transformation. It appears to stem from that the excessive amount of PCA inhibits appropriate cold welding for mechanical alloying. No other peaks besides alpha Ti and Al-3V were observed in the XRD result meaning that the cryogenic temperature successfully prevented contamination of oxygen or nitrogen forming oxides or nitrides, respectively.
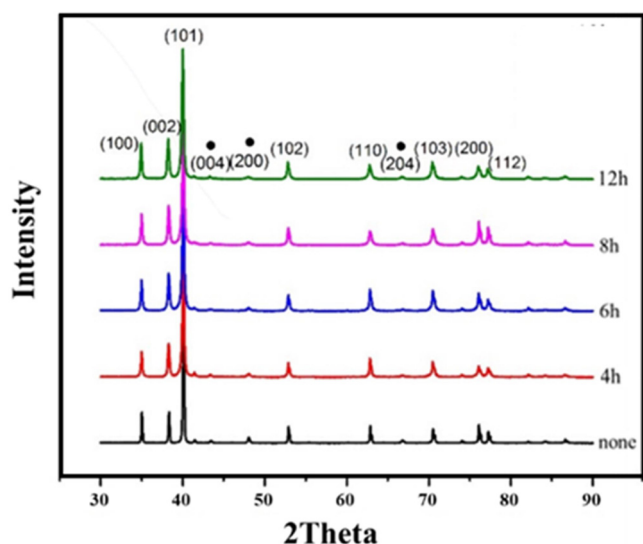

Fig. 1. XRD peak analysis of cryomilled powder depending on milling time

The grain size of cryomilled powder was determined by X-ray peak broadening analysis using the Scherrer equation:

$$D = \frac{k\lambda}{\beta_D \cos\theta} \tag{2}$$

Where D is the grain size in nm, λ is the wavelength of the radiation (1.54056Å for CuKα radiation), k is the shape constant

equals to 0.94, β_D is the peak width at half the maximum intensity and θ is the peak position. The grain size variation calculated using Scherrer equation depending on the cryomilling time is shown in Fig. 2.
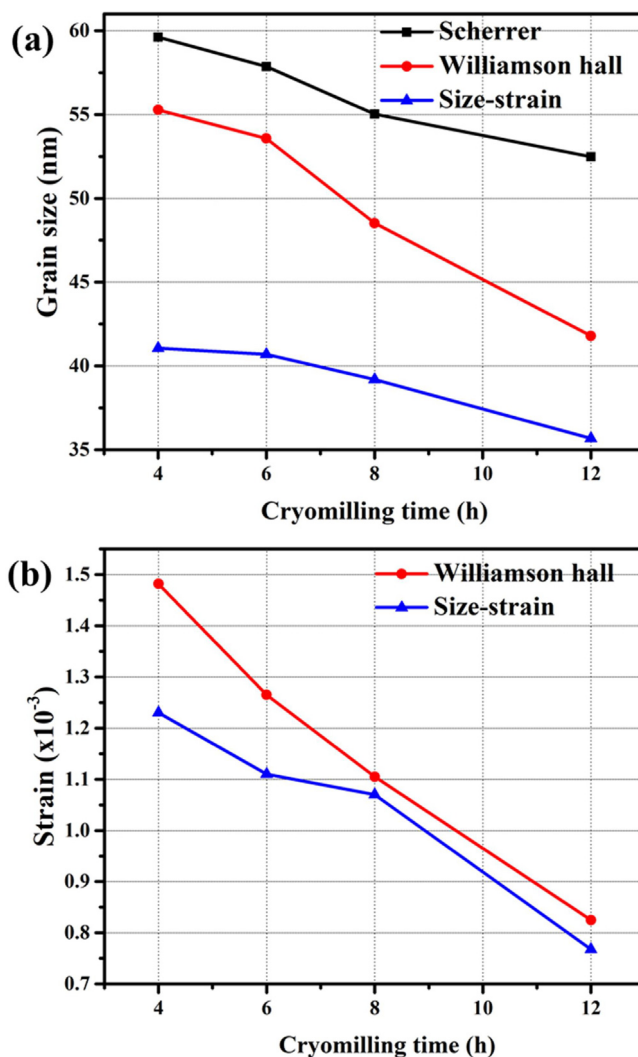

Fig. 2. Comparison of (a) grain size and (b) lattice strain data obtained from three different calculation methods

The grain size decreased with cryomilling time, and a minimum grain size of 52 nm was achieved after 12 hour cryomilling. The lattice strain induced by defects such as dislocations or lattice distortions generally results in XRD peak broadening [18]. Strain induced broadening arising from dislocations or lattice distortions is given by,

$$\varepsilon = \frac{\beta_s}{\tan\theta} \tag{3}$$

It is confirmed that the grain size varies with $1/\cos\theta$ whereas the strain varies with $1/\tan\theta$. The Williamson Hall plotting analysis is also suitable for calculating the grain size and lattice strain. So, using the strain induced line broadening β_s from eq. (3), the Scherrer equation in eq. (2) gives the following relations,

$$\beta_{hkl} = \beta_D + \beta_s \tag{4}$$

$$\beta_{hkl} = \left(\frac{k\lambda}{D\cos\theta}\right) + 4\varepsilon\tan\theta \qquad (5)$$

Where ε is the lattice strain. Rearranging eq. (5),

$$\beta\cos\theta = \left(\frac{k\lambda}{D}\right) + 4\varepsilon\sin\theta \qquad (6)$$

The eq. (6) represents the uniform deformation model where the strain was assumed to be uniform in all crystallographic orientations, thus considering the isotropic nature of the crystal, where all the material properties are independent of the measured direction.

The calculated grain size and lattice strain via Williamson Hall method were also plotted in Fig. 2. The grain size was 55.3 nm after 4 hour cryomilling, and 41.8 nm after 12 hour cryomilling. The grain size from the Williamson Hall analysis was smaller than that from the Scherrer equation. The lattice strain from W-H method also decreases with milling time. In the W-H method, the diffracting domains were isotropic and there was also micro-strain contribution. However, in cases of isotropic line broadening, a better evaluation of the size-strain parameters can be obtained by considering an average 'size-strain plot'. In this approximation, it is assumed that the 'grain size profile' is described by a Lorentzian function and the 'strain profile' by a Cauchy/Gaussian function [19]. Accordingly, we have,

$$\left(d_{hkl}\beta_{hkl}\cos\theta\right)^2 = \left(\frac{k\lambda}{D}\right)\left(d_{hkl}^2\beta_{hkl}\cos\theta\right) + 16\varepsilon^2 \qquad (7)$$

Where d_{hkl} depends on the d-spacing. Similar to the W-H method, this relationship from the SSP method was plotted to acquire the grain size and lattice strain as also shown in Fig. 2.

The grain size and lattice strain obtained from all three methods, Scherrer, W-H, and S-S, were summarized in Fig. 2. In the grain size, the calculation from S-S method shows lowest grain size values in average compared with other methods. In all methods, the grain size almost linearly decreases with increasing milling time. It means the grain size can be further refined by cryomilling more than 12 hours. The lattice strain data calculated by the W-H method was slightly higher than that from the S-S method for shorter cryomilling time than 8 hours. However, two methods show similar lattice strain values over 8 hours of cryomilling. The SSP model showed that the grain size and lattice strain reductions were more moderate than those obtained by the W-H method. The W-H method is not calibrated for the peak shape, while the S-S method takes account of shape difference because the XRD peaks are smooth and ideal through all the corrections.

Figure 3a shows a TEM micrograph of 8 hour cryomilled powder, and a histogram of grain size distribution measured from this TEM image is shown in Fig. 3b. As a result of image analysis, the average grain size from TEM image was 43.5 nm. For the 8 hour cryomilled powder, the grain size via Scherrer equation was 55.0 nm, via W-H plotting was 48.5 nm, and via S-S plotting was 39.2 nm. The size-strain plot method shows relative similar grain size than other methods. This means
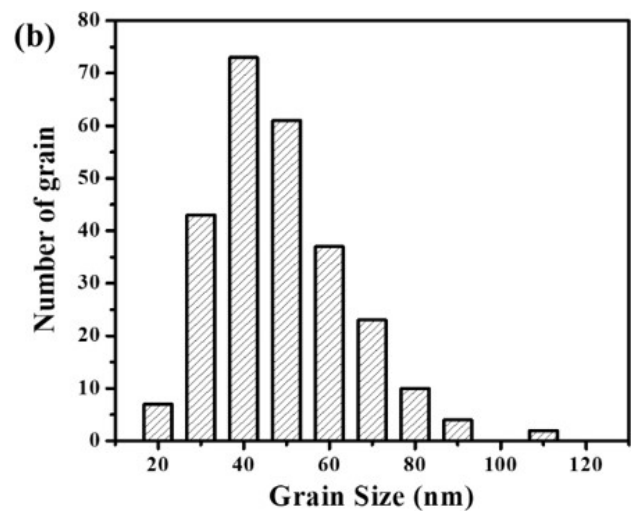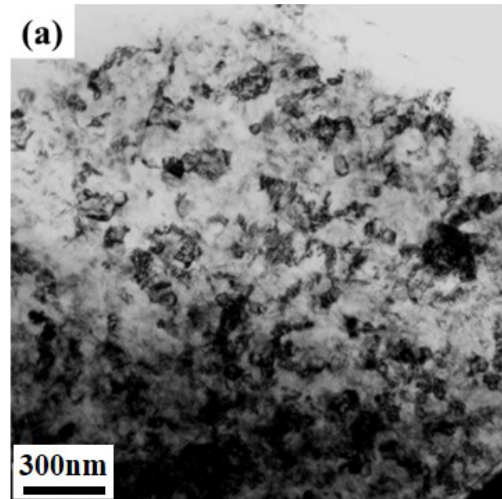

Fig. 3. (a) TEM micrograph and (b) grain size histogram measure from TEM micrograph of 8 hour cryomilled powder

the strain is not uniform and also had many high angle grain boundaries [20].

The accuracy of lattice strain is decide with similarity between calculation data and lattice parameter. The lattice parameter is calculated by following equations:

$$\sin^2\theta = \frac{\lambda^2}{4a^2}\left(h^2 + k^2 + l^2\right) \qquad (8)$$

Where h, k, l are Miller indices (calculated from the Bragg equation) and a is lattice parameter. In this research, the lattice parameters were calculated in the peaks which had maximum intensity.

The lattice parameter calculated from XRD peaks depending on the cryomilling time is shown in Fig. 4. When cryomilling time is increased, the lattice parameter decreases, and the lattice parameter became similar value to the original lattice parameter 2.95Å when cryomilled for 12 hours. The reason of reduction of lattice parameter and lattice strain is dislocation migration to grain boundary [21]. The strain and dislocation are heavily increased in early stage of cryomilling process, and some of them develop to a subgrain dislocation cells. Then, as cryomill-

1442

ing continues, the dislocations are re-arranged and develop to low angle grain boundary. The lattice parameter variation in Fig. 4 is close to the strain graph of W-Hall plotting method so that overall consideration shows the W-H method is appropriate to determine the grain size and lattice strain of this cryomilled Ti-6Al-4V powder.
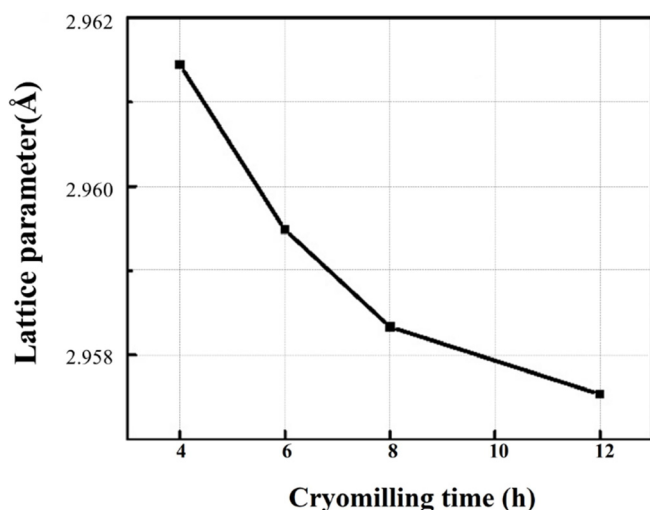

Fig. 4. Lattice parameters calculated from XRD peaks

4. Conclusions

Ti-6Al-4V powder was cryomilled to achieve nanocrystalline structure and characterized by XRD and TEM. The line broadening of Ti-6Al-4V powder was due to the small crystallite size and lattice strain. Various methods, the Scherrer equation, Williamson-Hall plotting method, and size-strain plotting method, were applied to analyze the line broadening. Considering relationship between the grain size and lattice strain, the Williamson-Hall plot was most appropriate calculating method for this cryomilled Ti-6Al-4V powder. The grain size from TEM microstructure and lattice parameter value are in good agreement with Williamson-Hall plotting method.

REFERENCES

[1] H. Gleiter, Acta Mater. **48**, 1 (2000).

[2] K.S. Kumar, H. Van Swygenhoven, S. Suresh, Acta Mater. **51**, 5743 (2003).

[3] C.C. Koch, Nanostruct. Mater. **9**, 13 (1997).

[4] H.J. Fecht, Nanostruct. Mater. **6**, 33 (1995).

[5] S.S. Yang, H.S. Kim, K.M. Lee, J.K. Lee, J. Korean Powder. Metall. Inst. **6**, 49 (1999).

[6] F. Sun, P. Rojas, A. Zúñiga, E.J. Lavernia, Mater. Sci. Eng. A **430**, 90 (2006).

[7] F. Sun, A. Zúñiga, P. Rojas, E.J. Lavernia, Metall. Mater. Trans. A **37**, 2069 (2006).

[8] O. Ertorer, T.D. Topping, Y. Li, W. Moss, E.J. Lavernia, Scr. Mater. **60**, 586 (2009).

[9] O. Ertorer, A. Zúñiga, T.D. Topping, W. Moss, E.J. Lavernia, Metall. Mater. Trans. A **40**, 91 (2009).

[10] O. Ertorer, T.D. Topping, Y. Li, W. Moss, E.J. Lavernia, Metall. Mater. Trans. A **42**, 964 (2011).

[11] Y. Sun, K, Kulkarni, A.K. Sachdev, E.J. Lavernia, Metall. Mater. Trans. A **45**, 2750 (2014).

[12] S.G. Pyo, H.H. Chung, S.J. Hwang, N.J. Kim, J. Korean. Powder. Metall. Inst. **5**, 98 (1998).

[13] J. He, E.J. Lavernia, J. Mater. Res. **16** (2001) 2724.

[14] F. Zhou, S.R. Nutt, C.C. Bampton, E.J. Lavernia, Metall. Mater. Trans. A **34**, 1985 (2003).

[15] Y. Xun, E.J. Lavernia, F.A. Mohamed, Metall. Mater. Trans. A **35**, 573 (2004).

[16] W. Dmowski, T. Egami, K.E. Swider Lyons, C.T. Love, D.R. Rolison, J. Phys. Chem. B **106**, 12677 (2002).

[17] Z. Zhang, F. Zhou, E.J. Lavernia. Metall. Mater. Trans. A **34**, 1349 (2003).

[18] V. Senthilkumar, P. Vickraman, M. Jayachandran, C. Sanjeeviraja, J. Mater. Sci. Mater. Electron. **21**, 343 (2010).

[19] J.D. Makinson, J.S. Lee, S.H. Magner, R.J. De Angelis, W.N. Weins, A.S. Hieronymus, JCPDS-International Centre for Diffraction Data 2000, Adv. XRay Anal. **42**, 407 (2000).

[20] A. Khorsand Zak, W.H.A. Majid, M.E. Abrishami, R. Yousefi, Solid State Sci. **13**, 251 (2011).

[21] S.R. Tousi. R.Y. Rad, E. Salahi, I. Mobasherpour, M. Razavi, Powder. Tech. **192**, 346 (2009).